TAO, Vol. 9, No. 3, 345-362, September 1998

Crustal Structure Beneath the Nanao Forearc Basin From TAICRUST MCS/OBS Line 14

Kirk D. McIntosh[1] and Yosio Nakamura[1]

(Manuscript received 6 March 1998, in final form 28 July 1998)

ABSTRACT

A velocity model constructed using ocean bottom seismometer (OBS) data collected along TAICRUST Line 14 indicates that the Ryukyu Arc basement (velocity > ~5 km/s) extends beneath the Nanao forearc basin to a depth of 18 to 20 km. Furthermore, our velocity model indicates that the Ryukyu Arc basement extends west to at least 122°E, near the west end of line 14, within about 50 km of the Coastal Range of eastern Taiwan. The westward extent of arc basement to 24°N, 122°E eliminates the possibility of a large northward transform offset of the trench as commonly shown. Beneath the Nanao Basin the depth to the base of this forearc crustal layer is consistent with the position of the thrust boundary between the subducting Philippine Sea Plate (PSP) and overlying Ryukyu Arc as determined by earthquake studies. In the western portion of the line the probable base of PSP crust appears to be at depths greater than 30 km. The velocity model is based on data recorded by seven, 4-component OBSs deployed at nominal 25 km spacing. The seismic energy source for the OBS data was a 20 airgun array operated from the R/V *Maurice Ewing*, which simultaneously collected deep-penetration multi-channel seismic reflection data. We constructed the velocity model using forward and inverse travel time modeling of reflected and refracted arrivals recorded at offsets of 0 to 95 km. The coincident MCS data were used to develop the starting model and the final model remains consistent with the sedimentary layering and basement structure evident in the MCS data set.

(Key words: Taiwan, Ryukyu, Subduction, Refraction, OBS)

1. INTRODUCTION

The island of Taiwan is generally considered the result of the collision of the Luzon Arc and the Eurasia continental margin (e.g., Chai, 1972; Suppe, 1981) or a paleo-Ryukyu Arc

[1]Institute for Geophysics, University of Texas, 4412 Spicewood Springs Rd., Bldg. 600 Austin, TX 78759-8500, USA

(Hsu and Sibuet, 1995) in Late Miocene or Pliocene times. Most models feature a trench-trench transform fault between the Manila and Ryukyu trenches that decreased in length through time, finally leading to the collision (e.g. Seno and Maruyama, 1984; Teng, 1990). Despite this general framework, the details of Taiwan's tectonic development and even the location and nature of the current structural and plate boundaries are not fully documented. A particularly complex area is the junction of the Coastal Range of eastern Taiwan and the Ryukyu Arc. This zone (Figure 1) is where the Philippine Sea Plate (PSP) changes from overriding the Eurasia Plate to subducting beneath the Eurasia Plate and the Ryukyu Arc. In this area some truly fundamental questions have remained unanswered. For example, how far west does the Ryukyu Arc extend, and is it offset by strike-slip or transform faults near Taiwan? Exactly how does the PSP change from overriding to subducting plate with respect to Eurasia? What is the position and geometry of the subducting plate boundary in the southwesternmost Ryukyu Arc?

Previous work based on marine and land geology, marine geophysics, and earthquake seismology has resulted in various tectonic interpretations of this area. Wu (1970, 1978) interpreted that the Ryukyu Trench is offset 50-100 km north between Gagua Ridge and Taiwan, while Rau and Wu (1995) interpret that the Ryukyu trench intersects Taiwan at 23.8° N. Kao *et al.* (1998) have studied earthquakes recorded by local and global networks to determine accurate hypocentral depths and source mechanisms. Their work suggests that the PSP is at 20-25 km beneath the Nanao Basin at 24° N but shallows significantly westward to possibly less than 5 km at 24° N, 122° E. Using multi-channel seismic reflection data (MCS), gravity data, and bathymetry, Lallemand *et al.* (1997) have proposed that the PSP is tearing between Taiwan and the Gagua Ridge such that the portion south of the tear collides with Eurasia while the portion to the north is free to subduct beneath the Ryukyu Arc and northern Taiwan. Schnrle *et al.* (1998) have interpreted that the Gagua Ridge has penetrated beneath the Ryukyu forearc causing basement uplift and widespread normal faulting. Ho (1986) and Hsu *et al.* (1996) have interpreted deformation of the Ryukyu Arc and Okinawa Trough along north to northwest oriented dextral slip faults on the basis of bathymetry and magnetic anomaly patterns.

In this area we use new MCS and ocean bottom seismometer (OBS) data to constrain the crustal structure and plate boundary configuration. In particular we present an interpretation of OBS data collected along TAICRUST Line 14. These data provide information on the velocity structure beneath the Nanao forearc basin, roughly parallel to the Ryukyu Arc-Trench system, from which general crustal structure can be inferred. Our velocity model provides information that bears directly on questions such as the extent of the Ryukyu Arc and the position of the subducting PSP beneath the forearc. We first describe the basic data, including acquisition, describe the model derived from interpreted OBS traveltimes, discuss the traveltime fit and resolution of the model elements, and finally discuss the implications of this model for the crustal structure and plate boundary configuration of the complex area.

2. DATA

Line 14 is part of the TAICRUST experiment, which took place in August and September, 1995. It is one of six lines in the project employing simultaneous MCS and OBS data acquisition. In this project OBS instruments from National Taiwan Ocean University (NTOU) and the University of Texas at Austin Institute for Geophysics (UTIG) were deployed and recovered from the R/V *Ocean Researcher I* while airgun source firing and MCS acquisition were performed with the R/V *Maurice Ewing*. Along line 14 (Figure 1) the mean airgun source interval was 36.8 m, the MCS trace spacing was 25 m, and OBS spacing was ~25 km. The source array was composed of 20 airguns with a total volume of about 8400 cu. in. Seven UTIG OBSs were used along line 14, recording three geophone channels, two horizontal and one vertical component, and a hydrophone. The sample interval was 4 ms and recording alias filters were set at 30 Hz and 50 Hz for the geophones and hydrophone, respectively. Data were recorded on SCSI disk drives. Source navigation was provided by continuous GPS coverage, and simultaneous GPS recording at a land station allowed for post cruise differential GPS (DGPS) navigation processing. This DGPS navigation dataset, was then used to relocate and orient the OBSs based on water wave arrivals.

The water depth along line 14 is progressively shallower from east to west crossing the segments of the Nanao Basin with rapid shoaling near the Taiwan margin. OBS positions and bathymetry are indicated in map view in Figure 1 and on the seismic line drawing in Figure 2. Except for OBSs 22 and 23, which are 5 km apart, the instrument spacing is 25 km.

Coherent arrivals recorded along line 14 can be observed to distances of at least 80 km on some of the seven record sections. In most cases, however, good arrivals occur at ranges less than 60 km. In Figure 3 record sections are plotted for all sections except OBS 22 (just 5 km from OBS 23). These plots cover a range of 120 km with 9 seconds of data displayed and a reduction velocity of 8 km, so the scales are identical and apparent velocities can be compared (Note: these records are not displayed in the correct spatial position relative to each other). It is clear from the generally asymmetric arrivals on these plots that the structure is not simple along the line. The primary cause of this asymmetry can be inferred directly from the record sections as excellent reflections from the base of the sedimentary section are visible and point to the highly variable basement structure. This rough structure is confirmed in the line drawing of the MCS data (Figure 2). The most extreme asymmetry is found in the OBS 24 section, which is centered at the edge of the central Nanao Basin (Figure 3d.). OBS 24 is also situated above a basement normal fault as is indicated by the offset in the reflection at the base of the sediments (3.8-4.5 s at ~zero offset; Figure 3d). This rough basement structure is significant for a number of reasons: a) apparent velocities, as measured on the record sections, are largely misleading, b) phase identification is complicated due to structurally induced slope variations, and c) some abrupt variations, especially under the deep angular Nanao Basin, appear to create shadow zones preventing continuous ray coverage.

In addition to first arrivals, several clear later arrivals have been identified, picked, and used in the travel time modeling. The best example of later arrivals is the top of basement reflection, as noted above, which can be identified on all but the OBS 20 record section. Other prevalent later arrivals can be seen on the OBS 26 record section (Figure 3f). The arrivals picked at the farthest offsets are from the OBS 24 record section. Figure 4 shows a portion of this section with shots 30-110 km west of the instrument. Here the first arrival is clear to -85 km and a later arrival, interpreted as a reflection from the base of the PSP crust, *i.e.*, PmP, has been picked from -65 to -95 km. These and several other arrivals help determine the deeper

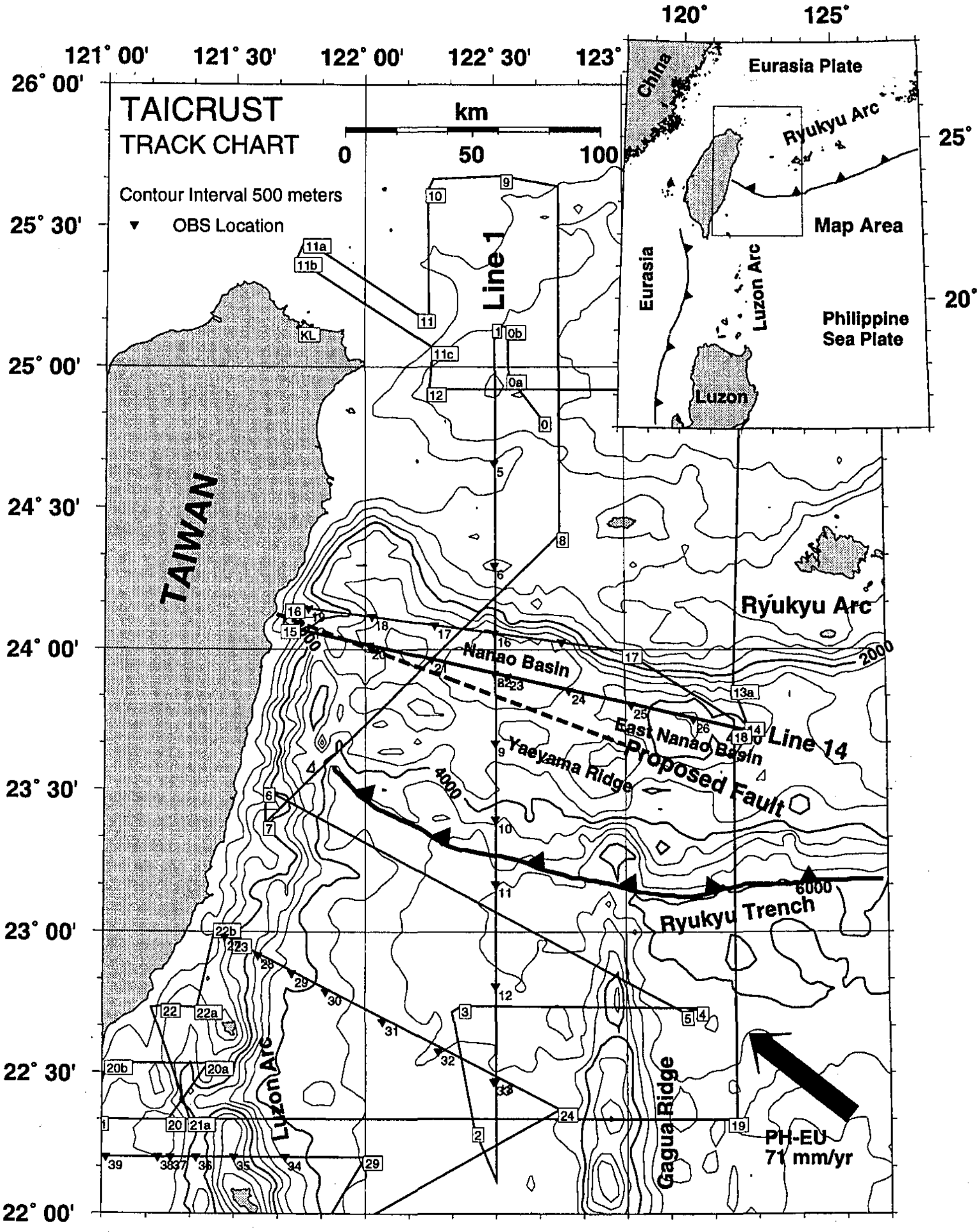

Fig. 1. Bathymetric map of study area offshore eastern Taiwan with inset map showing regional geographic and tectonic context. The TAICRUST track lines are shown for this area with lines 1 and 14 labeled. OBS positions are also marked and labeled. The location of the tear fault in the Philippine Sea Plate as proposed by Lallemand *et al.* (1997) is marked. Plate motion vector is from Seno *et al.* (1993).

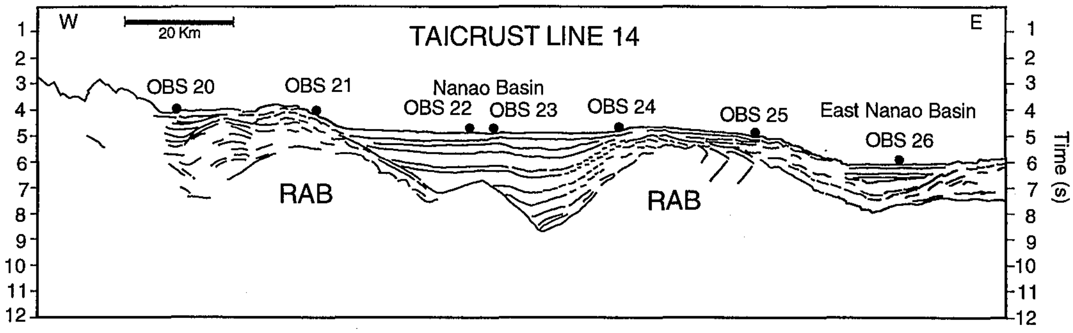

Fig. 2. Simplified line drawing of the Line 14 MCS data. This figure shows the variable thickness and bedding character of the sedimentary sections and the structural relief at the top of the basement. RAB=Ryukyu Arc basement. The OBS positions are marked and labeled along the line.

structure along this profile.

The MCS data collected along line 14 provide a helpful perspective in interpreting the OBS data and were also used to construct the starting model for travel time modeling. As seen in Figure 2, the top of the Ryukyu Arc basement (marked RAB) is essentially acoustic basement. However, the sedimentary bodies above basement vary significantly along the profile. As noted by Schnrle *et al.* (1998) the sediments of the western Nanao Basin are largely non-deformed. Toward the deeper portion of the basin and onto the basement high to the east, normal faults are prevalent in the sediments and penetrate into the eastern part of the basement high. Sediments of the East Nanao Basin show three depositional sequences (Schnrle *et al.*, 1998) and document additional normal faulting, except in the shallowest part of the section. At the western end of the profile there is a deformed sedimentary body overlying basement but below the little-deformed sediments of the Nanao Basin. This sedimentary body, just west of the Nanao Basin, likely is formed from the accretionary prism material of the Yaeyama Ridge as interpreted on an intersecting MCS profile by Lallemand *et al.* (1997). This deformed unit and the underlying arc basement both have clear westward dip between OBS 20 and 21 positions. West of this area the seafloor becomes rough and rapidly shallower. The absence of coherent reflections in this zone approaching Taiwan and the rough seafloor indicate intense deformation.

3. OBS TRAVEL TIME MODELING

The crustal velocity model was constructed using a combination of 2D travel time inversion and forward modeling, both employing the RAYINVR code (Zelt and Smith, 1992). The general process for modeling occurred as follows:

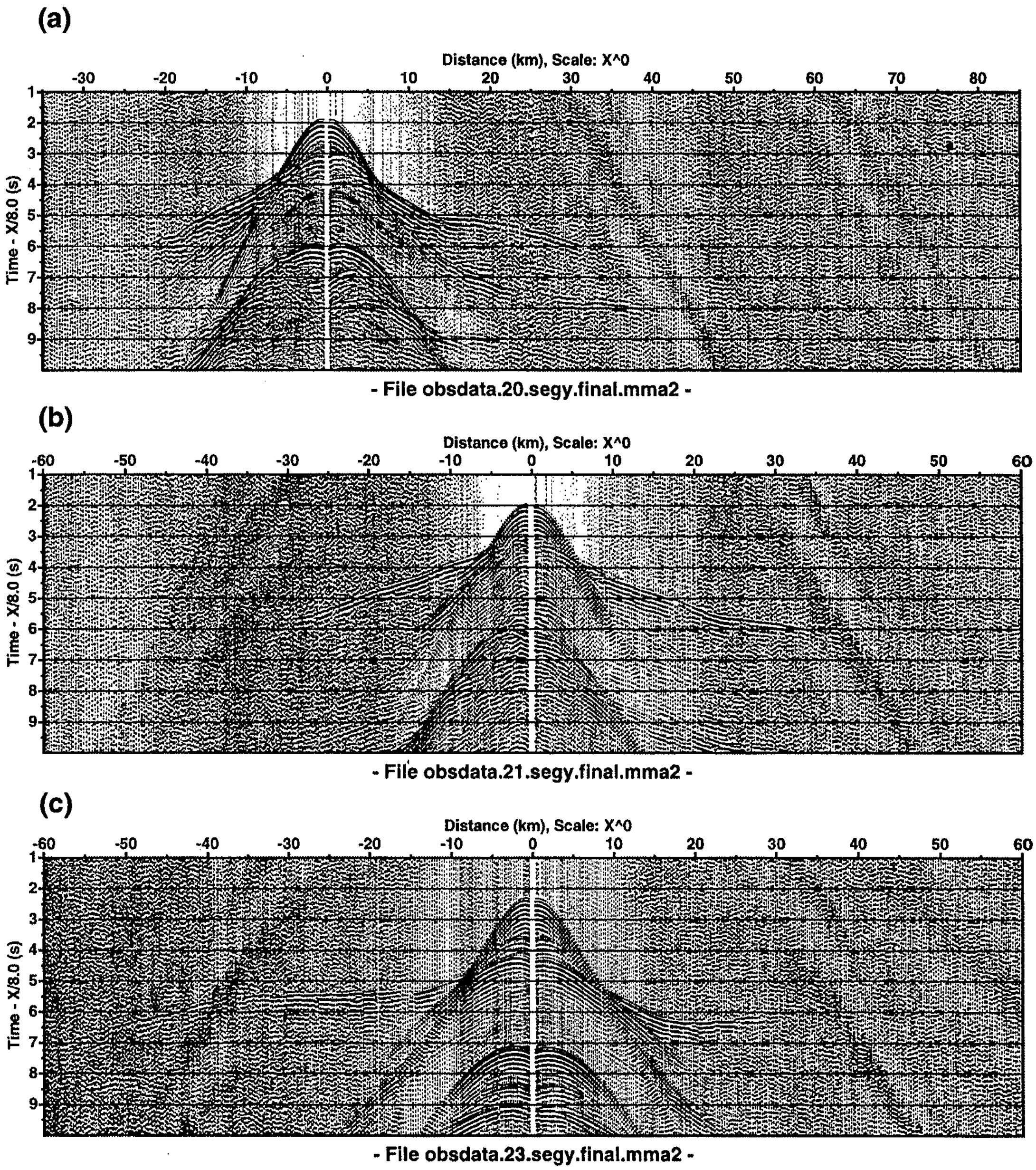

Fig. 3. Displays of record sections from OBSs 20, 21, 23, 24, 25, and 26 (parts a-f). In each plot a total length of 120 km is shown and a reduction velocity of 8 km/s was used. We used a five trace mix, a 3-12 Hz bandpass filter, and a 5 second AGC to create the displays. Every sixth trace is shown. See text for further description.

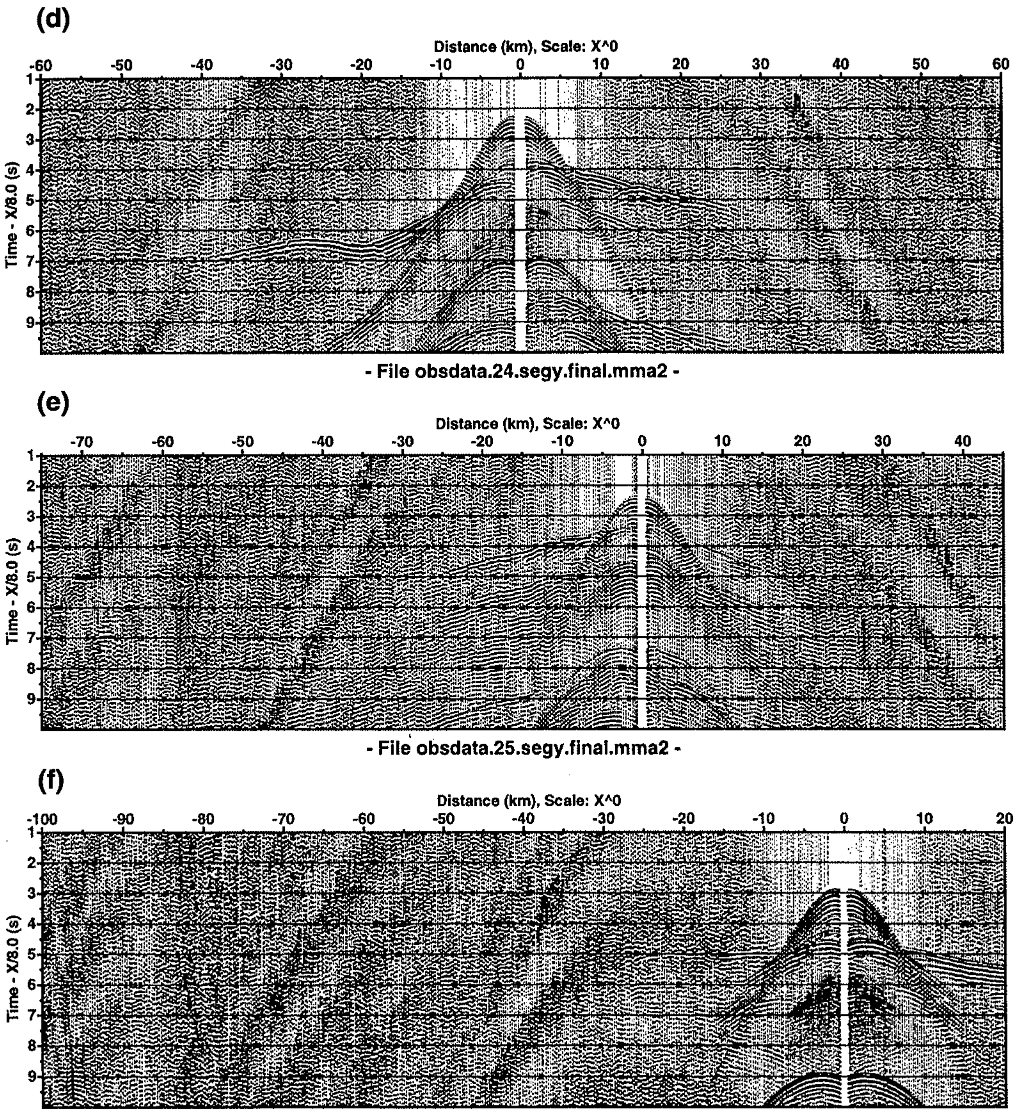

Fig. 3. (continued)

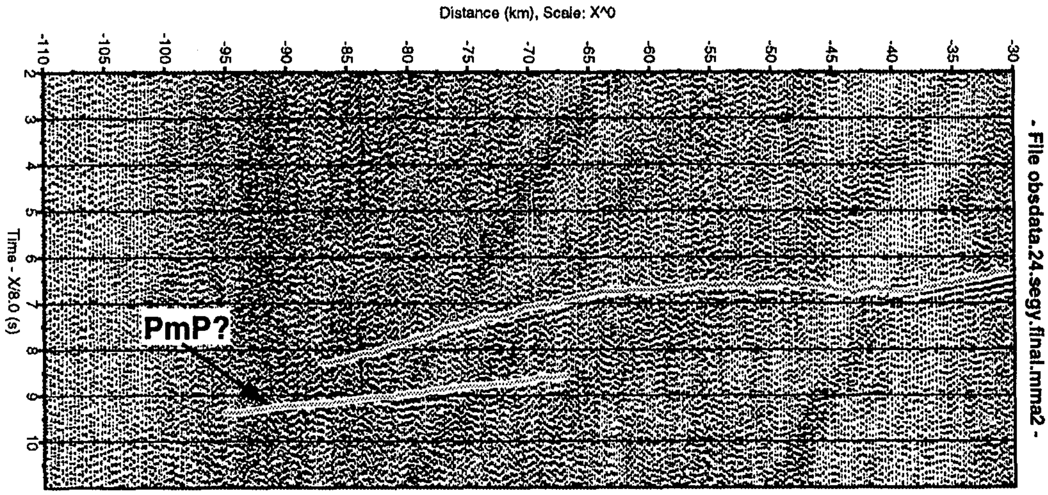

Fig. 4. Portion of OBS 24 record section showing farthest offset first arrivals and a prominent later arrival. Both of these arrivals are marked by our picks. The later arrival is interpreted here as PmP, the reflection from the base of the Philippine Sea Plate.

1. Pick arrivals on the OBS records and make preliminary phase designations.
2. Pick basement and the top of older, or more deformed, sediments on the MCS record section.
3. Use reflections and refractions in the Nanao Basin, where layers are nearly horizontal to estimate sediment velocities and use apparent velocity of portions of OBSs 24 and 26 to estimate upper basement velocity.
4. Convert picked horizons to depth and assign the estimated velocity distribution.
5. Perform travel time inversion or forward modeling, beginning with the shallowest layer and work downward when fit becomes acceptable (in general fit is acceptable when rms misfit is < uncertainty and χ^2 error is < 1).

The shallow intra-sediment boundary position was refined by modeling reflections only, while the basement surface was determined by using both the clear reflection arrival, to zero offset (Figure 3), and the associated sedimentary refracted arrivals. After we accurately determined the basement surface and sedimentary velocities, we analyzed arrivals turning in the basement layers and, in a few cases, large aperture reflections. As noted above, it was difficult to differentiate between changes in the top of basement structure (and sediment thickness) versus changes in basement velocity on the basis of apparent velocity. In fact, the early modeling simply employed a large gradient in the basement velocity. This result showed that most of the arrival asymmetry is due to the top basement structure rather than abrupt vertical or lateral velocity variations. Eventually we determined that a two-layer crustal velocity structure with moderate gradients produced a better fit to the crustal refracted arrivals. With good arrivals generally limited to less than about 60 km, the velocity structure is well determined to about 15-20 km depth and the geometry at base of these layers and deeper layers is roughly determined by reflected arrivals.

The resulting velocity model is shown in Figure 5. Sediment velocities vary from 1.6 km/s at the seafloor to over 3 km/s in the deepest part of the Nanao Basin and in most of the older, deformed sediments at the west end of the line. Velocity at the top of the basement, crustal layer C1, is ~5 km/s (as low as 4.8 km/s and as high as 5.5 km/s). There appears to be a relatively strong gradient in the velocity (although not controlled by amplitude modeling) in this upper basement layer, with velocity approaching 6 km/s at its base. We interpret a thicker basement layer below this, crustal layer C2, on the basis of a slight velocity increase but an apparent decrease in velocity gradient. Here the velocities vary from ~ 6 km/s to 6.5 km/s. The base of layer C2 is only partially determined using reflection picks from OBSs 22, 24, and

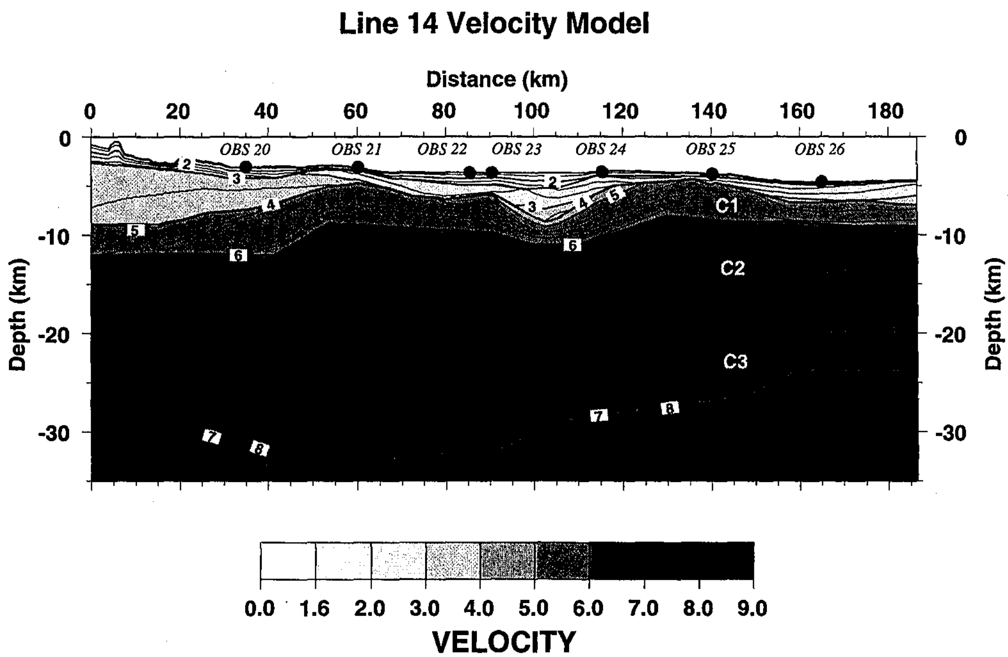

Fig. 5. Crustal velocity model based on OBS traveltime modeling. Basement crustal layers labeled C1 and C2 are interpreted as part of the Ryukyu Arc while layer C3 is more probably the subducting Philippine Sea Plate. The velocity contour interval is .25 km/s. The boundaries of the calculated velocity model are shown as heavy black lines.

26. The underlying layer C3 is shown to thicken significantly to the west, but it is poorly resolved and perhaps should be subdivided into two layers. The base of layer C3 is marked by good arrivals interpreted as reflections on OBSs 24 and 26 (Figures 3 and 4). The velocity in this layer is assumed to be ~6.5 km/s as no clear arrivals turning within it have been identified. The mantle velocity of 8 km/s shown in Figure 5 below layer C3 is also assumed and has not been determined by modeling.

4. TRAVELTIME FIT AND MODEL RESOLUTION

4.1 Traveltime Fit

As always we would like to know how good the model is and what parts of the model are better constrained than others. To convey this information we first present diagrams showing observed and calculated travel times for each instrument (Figure 6). In this output from program RAYINVR (Zelt and Smith, 1992), the calculated travel times appear as solid lines and the observed times appear as vertical lines proportional in height to the pick uncertainty. These figures are useful because they show the travel time fit, and they also indicate which arrivals are prevalent in the dataset. They also show which arrivals have been used to determine the poorly constrained deep layers of the model.

Arrivals 2.2 and 3.1. All instruments include a reflection picked within the sedimentary cover (arrival 2.2). The uncertainty for this pick is low, so the pick marks are about the same dimension of the lines marking the calculated travel times, thus they are largely masked by the calculated travel times in Figure 6. The total rms misfit for this arrival is .023 s. All instruments also recorded refracted arrivals through the lower part of the sedimentary section (arrival 3.1). As in the case of the reflection (2.2), these arrivals were picked with great precision on the broader band hydrophone records, so the picks are also largely masked by the calculated arrival in this display. The total rms misfit for this arrival is .053 s.

Arrival 3.2. This is the reflection from the top of the Ryukyu arc basement. It was picked on the MCS section and picked on all but OBS 20. As above the uncertainty was estimated at ~ .05 s picking on the hydrophone record, so picks are masked in this display. The total rms misfit for this arrival is .037 s.

Arrivals 4.1 and 5.1. These two phases, propagating through two layers of the Ryukyu Arc basement (layers C1 and C2), are the most prevalent arrivals recorded along line 14. As noted above, due to the rough basement surface it was difficult to distinguish between these two arrivals. There appears to be only a change in the velocity gradient separating these layers and, as expected, there is no prominent reflection produced at their interface. The total rms misfit for arrivals 4.1 and 5.1 are .078 s and .111 s, respectively.

Arrivals 5.2 and 6.2. These two reflected arrivals are present on many of the records but not consistently along the line. There is significant uncertainty in both making the picks and in

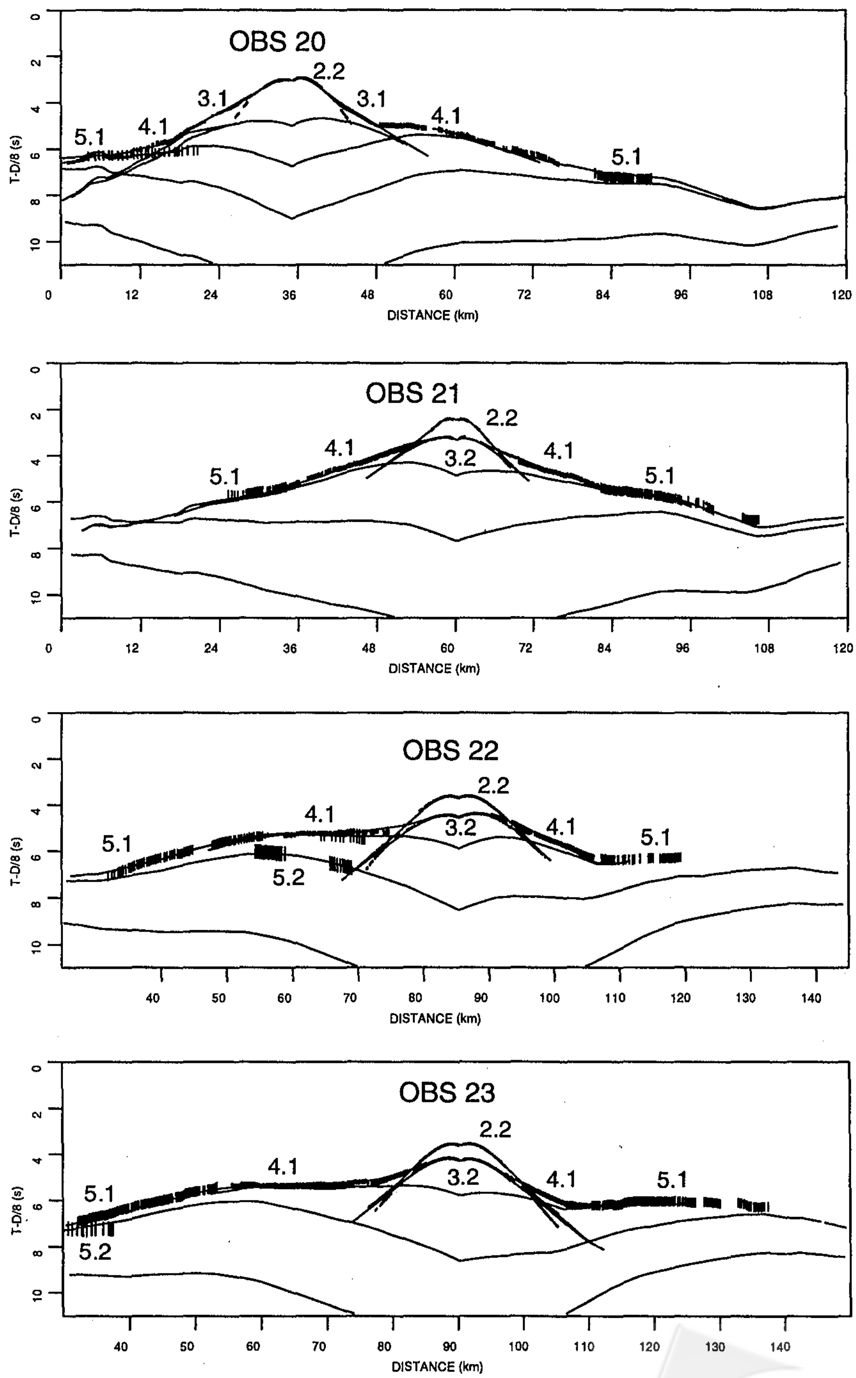

Fig. 6. (to be continued)

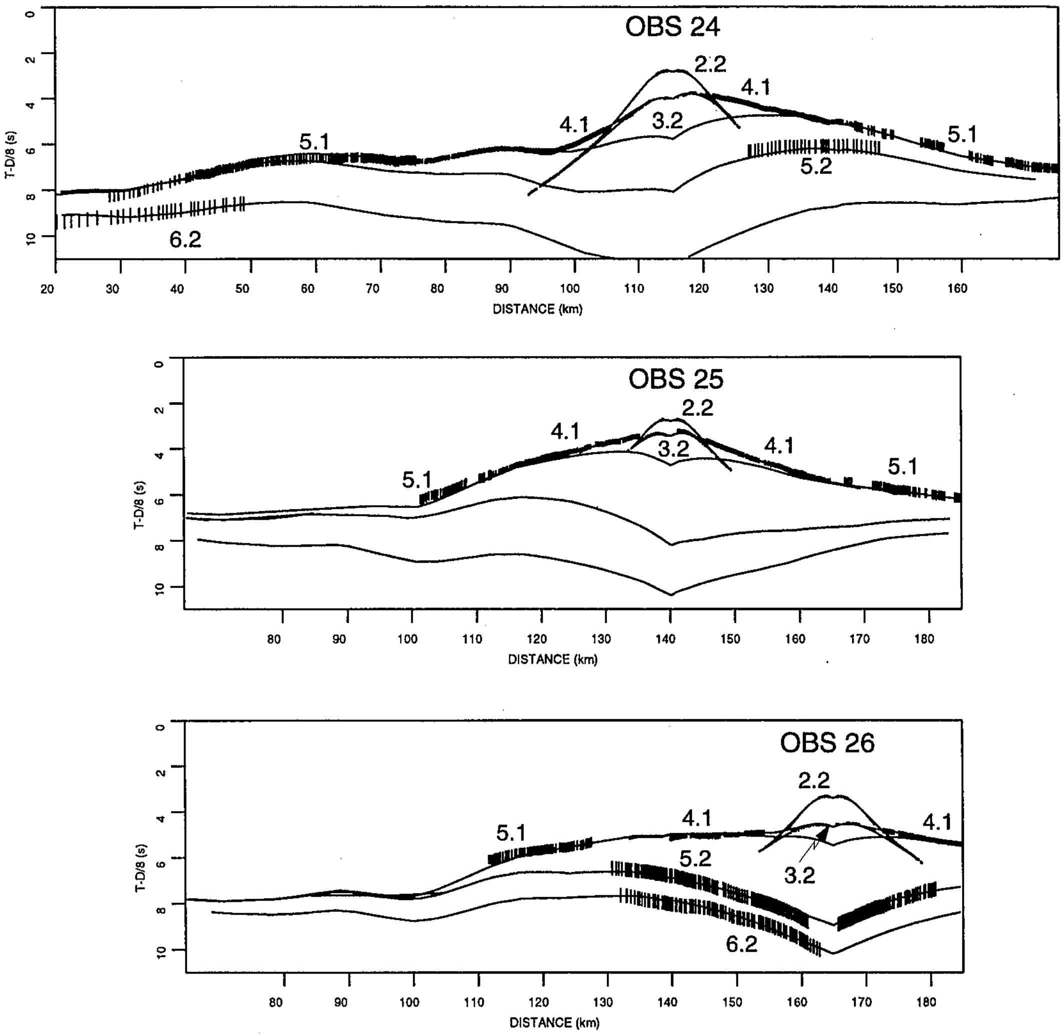

Fig. 6. Diagrams for each OBS showing observed and calculated travel times. The picked arrivals are marked by vertical lines proportional to the estimated uncertainty and the calculated arrivals, from the final model, are shown with solid lines. The picked arrivals are labeled (consistent with the RAYINVR program of Zelt and Smith, 1992) by layer number and arrival type (*e.g.*, 2.1 is a ray that turns in layer 2 and 2.2 is an arrival that reflects from the bottom of layer 2). Each diagram covers the same portion along the line as the corresponding record section shown in Figure 3 and all plots use a reduction velocity of 8 km/s.

assuring that the picks correspond to the same boundary on all instruments due to the 25-km instrument spacing. Nevertheless, arrival 5.2 is picked on 3 records and appears to document some deep structural features. Arrival 6.2 is picked on two records. For arrivals 5.2 and 6.2, rms misfit is .094 s and .105 s, respectively; the estimated uncertainty on the picks, due primarily to noise and the relatively long period (at low frequency), was ~.300 s.

4.2 Model Resolution

In addition to travel time misfit, model resolution is a statistical measure of how well the model is supported by the data. To a large extent the resolution indicates the ray coverage of the model, but the actual resolution estimates also depend on the parametrization of the model. In general the number of model parameters (boundary and velocity nodes) used is a tradeoff between traveltime fit and model resolution (Zelt and Smith, 1992); more model parameters may lead to a better travel time fit, but a greater number of parameters will not be as well resolved. Our model parametrization was not tested extensively for optimum model resolution, but velocity nodes at 1/2 the OBS spacing is generally considered reasonable (Zelt and Smith, 1992). Due to the MCS data and good reflected and refracted arrivals in the sedimentary section, the shallow structure is well constrained. Typical resolution values for the top of the basement boundary are 0.5 to 0.99, with values of 0.5 or greater considered well resolved (Holbrook *et al.*, 1994). The critical part of the model along line 14 is the sub-sedimentary crustal velocity structure. To present an idea of the model resolution here we posted the resolution values for layer C1 and C2 velocity nodes (top of layer only) on a diagram of the layer structure (Figure 7). For both layers it is clear that the ends of the model are poorly resolved, but the central portion, from ~40 km to ~165 km, is reasonably well resolved with values at or just below 0.50. As noted above, the base of layer C2 is determined by reflections picked on three of the OBS records; the reflection points along the boundary are marked by heavy lines along portions of the boundary (Figure 7). The resolution of the base of layer C2 nodes is posted just below the boundary. It is clear that the boundary is well resolved only between 140 km and 165 km. The base of layer C3 is well resolved only in the vicinity of OBS 26 due to reflections at near offsets. The portion of this boundary determined by the reflection from OBS 24 is marked by the heavy line at ~65-90 km. The low resolution here is due to relatively low ray density to this single instrument at large offset. However, we have reasonably good confidence in this pick because it is supported by a conjugate arrival on OBS 20 that has been identified but not picked due to its limited extent.

5. VELOCITY MODEL INTERPRETATION

The Nanao Basin lies at the base of a steep slope from the crest of the Ryukyu Arc. It is clear from TAICRUST MCS/OBS line 1, which crosses line 14 at OBS 22 (Figure 1), that the Ryukyu Arc basement underlies the Nanao Basin (Schnürle *et al.*, 1998). Thus we interpret that crustal layers C1 and C2 represent the seaward extension of the Ryukyu Arc crust. Our model (Figure 5) features an upper, sub-sedimentary, crustal layer with velocities 5-5.8 km/s (C1) and a thicker middle or lower crustal layer with velocities 6-6.6 km/s (C2). The closest

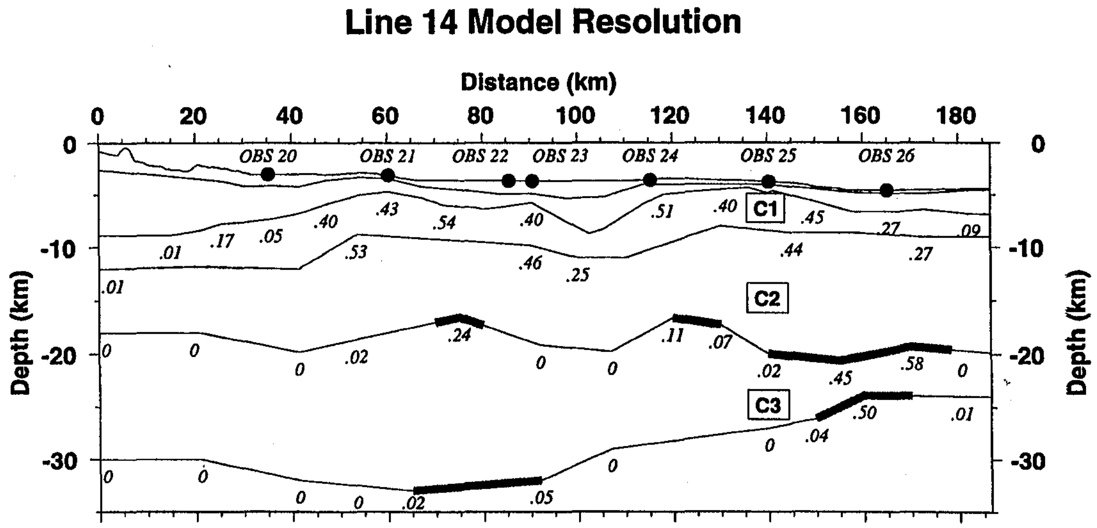

Fig. 7. Resolution estimates of our crustal velocity model. As described in the text, the numbers posted for layers C1 and C2 are for resolution of the velocity nodes at the tops of those layers. Numbers posted in and below layer C3 indicate the resolution of the model boundary at the top and bottom of C3. The heavy lines mark reflection points for arrivals used to constrain the top and bottom of C3. As expected, resolution increases substantially near the designated reflection points. Although resolution is not posted for the shallow boundary nodes, the top of C1 is well resolved with values typically 0.7-0.99.

previous measurement of forearc velocity is by Murauchi *et al.* (1968) ~500 km to the northeast along their profile 17. This profile indicated sub-sedimentary forearc velocities of 5.03 km/s and 6.43 km/s in two crustal layers. Other comparable crustal velocities were calculated by Lee *et al.* (1980) 5.5 km/s and 6.3 km/s in the Okinawa Trough, and Hirata *et al.* (1991) estimated velocities of 4.5-6 km/s and 6.2-6.4 km/s in the upper ~10 km on a profile crossing the Okinawa Trough and Ryukyu Arc. An important observation about layers C1 and C2 is that their presence is clear at least between x=30 km and x=170 km where structure and velocity are well resolved.

The nature of crustal layer C3 is not as well determined from the line 14 data set because the deeper velocity cannot be calculated and reflected arrivals are not consistently present on all records. However, on the basis of intersecting line 1 velocity models, which indicate the plate boundary at ~18-22 km beneath the Nanao Basin (Wang *et al*, 1996; McIntosh *et al.*, 1997), and hypocentral depths of low angle thrust earthquake events at 15-25 km in this area (Kao, 1998), it is likely that the boundary between the subducting PSP and the Ryukyu Arc is near the C2-C3 interface. This implies a forearc basement crustal thickness of ~13 km in the central and eastern portion of the line. In the western portion of the line we have not picked refracted or reflected arrivals to mark the base of layer C2, so the velocity model boundary there is only approximate. We note that this strike transect is not expected to measure the full arc crustal thickness due to its outboard or seaward position. In fact the top of the arc basement is generally below 5 km along this profile, whereas across the adjacent arc to the north it is at depths of 0.5 to 1.0 km a difference of over 4 km. This difference, plus the expected crustal root beneath the arc account for our ~13 km crustal thickness versus an expected arc thickness > 20 km.

Another feature of the eastern part of this model is that there is a bump at 110-140 km as indicated by reflections observed on OBS 24 and 26 records. This apparent structure is below the basement uplift that separates the Nanao Basin and the East Nanao Basin. The overlying velocity structure is reasonably well resolved with little change across this zone, so the bump is unlikely to result from a velocity problem; it is most likely a direct indication that the Gagua Ridge has penetrated beneath the forearc basement.

A significant element of the velocity model is the apparent thickness changes in layer C3. As noted above, the top of C3 is undetermined in the western portion of the line and its base is determined by reflections from OBS 24 and 26 record sections as shown in Figure 7. With this sparse coverage it is possible that the top of C3 is significantly too high in the western part of the model or that C3 is composed of two layers which we have been unable to distinguish. If layer C3 represents the PSP crust, as suggested above, then the thickness variations have important implications. In the vicinity of OBS 26, where reflections mark the interpreted top and bottom of the layer, it is unusually thin for oceanic crust, about 5 km. In contrast, our model shows that it may be thicker than oceanic crust, ~10 km thick, beneath OBS 24 and may thus support the presence of the Gagua Ridge. The anomalous thickness, approaching 15 km, at x=60-80 km is the most likely area for an unrecognized layer to be present. On the other hand, some crustal thickening may be expected due to close proximity of the former North Luzon Arc.

6. DISCUSSION AND CONCLUSIONS

The principal contribution of this work is to present the velocity model (Figure 5), a piece of fundamental information that can be used in making an integrated interpretation for the region. Below we make some observations given these basic data:

1. East of x=60 km nearly all of the sedimentary section velocity is < 3 km/s. The exceptions are in the deepest part of the Nanao Basin, 3+ km below the seafloor, and in the deepest part of the East Nanao Basin, where apparently older sedimentary rocks are present (Schnürle *et al.*, 1998). In contrast, west of x=60 km the sedimentary section reaches velocities > 3 km/s at 1-1.5 km below the seafloor, and this higher velocity sedimentary body thickens westward. This observation supports the interpretation that some of these rocks are derived from the accretionary prism (Yaeyama Ridge), which clearly overlies the seaward part of

the Ryukyu Arc basement along TAICRUST Line 1 to the east (Schnürle *et al.*, 1998).

2. Layers C1 and C2 are part of the Ryukyu forearc basement, which extends beneath the forearc basins. The documented presence of this rock body, velocity 4.8-6.5 km/s, westward to x=30 km, or 24°N, 122°E, marks the minimum extent of the Ryukyu Arc toward Taiwan and the Luzon Arc.

3. With the combined basement thickness of ~9-13 km, a sedimentary section, and 2-4 km water depth, the position of the PSP-Ryukyu subduction plate boundary thrust lies at approximately 18 to 20 km depth beneath Line 14. This is in good agreement with hypocentral depths for interface seismic events modeled by Kao *et al.* (1998) beneath the central Nanao Basin and consistent with TAICRUST Line 1 models (Wang *et al.*, 1996; McIntosh *et al.*, 1997). However, this relatively deep position of the boundary, together with the westward extent of the arc basement, and the morphologic expression of the trench extending west to 23°30' N, 121°50'E (Figure 1) indicates that there is no single, large northward offset of the trench or main thrust zone as suggested by Wu (1970, 1978). We note that our model does not rule out more distributed deformation of the forearc along northwesterly trending dextral slip faults as interpreted by Hsu *et al.* (1996).

4. West of Nanao Basin our estimated position of the plate boundary thrust (PSP-Ryukyu) at the layer C2-C3 interface apparently does conflict with the position estimated by Kao *et al.* (1998). We don't have direct evidence for the position of this boundary, but the top of the basement is reliably marked at ~ 8 km depth at 24°N, 122°E. The base of layer C2 is expected 9 to 13 km deeper or 17-21 km depth at this point. This is 10+ km deeper than indicated by isodepth contours from Kao *et al.* (1998). We also point out that 35 km to the east, where the top and base of layer C3 are determined, their depths are 17 km and 32 km, respectively, also indicating a relatively deep position for the PSP. If this interpretation is correct, it suggests that the shallow interface seismic event I17 modeled by Kao *et al.* (1998) may be an upper plate event, or, alternatively, the plate boundary interface and PSP crust may become abruptly shallower somewhat west of 122°E.

5. Schnürle *et al.* (1998) interpret that the basement high that separates the Nanao Basin from the East Nanao Basin is due to Gagua Ridge penetration beneath the Ryukyu forearc. Our velocity model shows an apparent bump in the top of crustal layer C3, which we expect is the subducting PSP. Thus our result appears to confirm the northward penetration of the Gagua Ridge beneath the Ryukyu forearc.

6. The presence of a tear in the PSP as proposed by Lallemand *et al.* (1997) (Figure 1) cannot be directly confirmed or rejected by our results from Line 14. However the top of layer C3 at ~20 km depth along Line 14 requires an average dip just over 7° in the 80 km distance from the trench (at 122.5°E), thus a fault is not required south of Line 14 as proposed.

Acknowledgements We thank the captain and crew of the R/V *Ocean Researcher I* who were so helpful in the OBS deployments and recoveries and were patient and cooperative through the five typhoons that made this cruise a real challenge. Tan-Kin Wang, Stephane Operto, Chao-Shing Lee, Glen Caglarcan, Jack Pitter, Tain-Syh Liu, and Julia Liu participated in the cruise and provided valuable assistance. We also thank the captain and crew of the R/V Maurice Ewing who provided an excellent energy source for our OBS work and worked hard to coordinate the OBS and MCS data acquisition. The differential GPS data and MCS data were processed by Philippe Schnrle and provided for our use by Philippe and Char-Shine Liu. Our work was supported by National Science Foundation grant OCE-9417411.

REFERENCES

Chai, B. H. T., 1972: Structure and tectonic evolution of Taiwan. *American Journal of Science* **272**, 389-422.

Hirata, N, H. Kinoshita, H. Katao, H. Baba, Y. Kaiho, S. Koresawa, Y. Ono, and K. Hayashi, 1991: Report on DELP 1988 Cruises in the Okinawa Trough Part 3. Crustal structure of the southern Okinawa Trough. *Bulletin of the Earthquake Research Institute University of Tokyo,* **66**, 37-70.

Ho, C. S., 1986: A synthesis of the geologic evolution of Taiwan. *Tectonophysics,* **125**, 1-16.

Holbrook, W. S., E. C. Reiter, G. M. Purdy, D. Sawyer, P. L. Stoffa, J. A. Austin, J. Oh, and J. Makris, 1994: Deep structure of the U.S. Atlantic continental margin, offshore South Carolina, from coincident ocean bottom and multichannel seismic data. *J. Geophys. Res.,* **99**, B5, 9155-9178.

Hsu, S. K. and J. C. Sibuet, 1995: Is Taiwan the result of arc-continent or arc-arc collision?, *Earth and Planetary Science Letters,* **136**, 315-324.

Hsu, S. K., J. C. Sibuet, S. Monti, C. T. Shyu, and C. S. Liu, 1996: Transition between the Okinawa Trough backarc extension and the Taiwan collision: New insights on the southernmost Ryukyu subduction zone. *Marine Geophys. Res.,* **18**, 163-187.

Kao, H., S. S. J.. Shen, and K..F. Ma, 1998: Transition from oblique subduction to collision: earthquakes in the southernmost Ryukyu arc-Taiwan Region, *J. Geophys. Res.,* **103**, 7211-7229.

Lallemand, S. E., C. S. Liu, and Y. Font, 1997: A tear fault boundary between the Taiwan orogen and the Ryukyu subduction zone. *Tectonophysics,* **274**, 171-190.

Lee, C. S., G. G. Shore, Jr., L. D. Bibee, R. S. Lu, and T. W. C. Hilde, 1980: Okinawa Trough: origin of a back-arc basin. *Marine Geology,* **35**, 219-241.

McIntosh, K. D., Y. Nakamura, F. King, W. T. K., and C. S. Liu, 1997: OBS data support interpretation of tear in Philippine Sea Plate east of Taiwan. *Supplement to EOS, Transactions, AGU 1997 Fall Meeting,* **78**, 46, 718.

Murauchi, S., N. Den, S. Asano, H. Hotta, T. Yoshii, T. Asanuma, K. Hagiwara, K. Ichikawa, T. Sato,and W. J. Ludwig, 1968: Crustal structure of the Philippine Sea, *J. Geophys. Res.,* **10**, 3143-3171.

Rau, R. J., and F. T. Wu, 1995: Tomographic imaging of lithospheric structures under Taiwan. *Earth and Planet. Sci. Lett.,* **133**, 517-532.

Schnürle, P., C .S. Liu, S. E. Lallemand, and D. Reed, 1998: Structural insight in the south Ryuku margin: effects of the subducting Gagua Ridge. *Tectonophysics,* **288**, 237-250.

Seno, T., and S. Maruyama, 1984: Paleogeographic reconstruction and origin of the Philippine Sea. *Tectonophysics,* **102**, 53-84.

Seno, T., S. Stein, and A. E. Gripp, 1993: A model for the motion of the Philippine Sea Plate consistent with NUVEL-1 and geologic data. *J. Geophys. Res.,* **98**, 17941-17948.

Suppe, J., 1981: Mechanics of mountain building and metamorphism in Taiwan. *Geol. Soc. China Mem.*, **4**, 67-89.

Teng, L.S., 1990: Geotectonic evolution of late Cenozoic arc-continent collision in Taiwan. *Tectonophysics,* **183**, 57-76.

Wang, T. K., K. D. McIntosh, Y. Nakamura, and C. S. Liu, 1996: OBS data refraction survey and imaging offshore eastern Taiwan. *Supplement to EOS, Transactions, AGU 1996 Fall Meeting,* **77**, 720.

Wu, F. T., 1970: Focal mechanisms and tectonics in the vicinity of Taiwan. *Bull. Seism. Soc. America,* **60**, 2045-2056.

Wu, F. T., 1978: Recent tectonics of Taiwan. *J. Physical Earth,* **26**, Suppl., S265-S299.

Zelt, C. A., and R. B. Smith, 1992: Seismic traveltime inversion for 2-D crustral velocity structure. *Geophys. J. International,* **108**, 16-37.